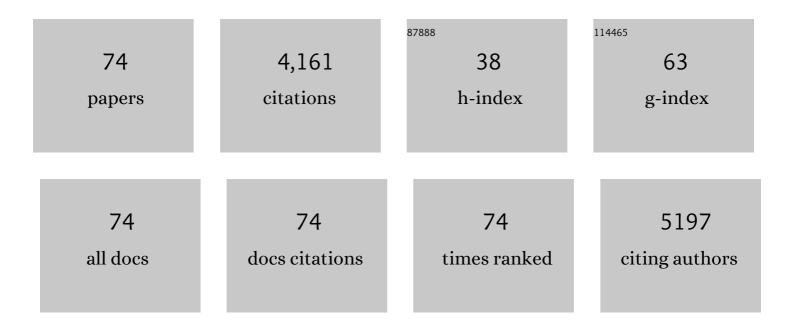
List of Publications by Year in descending order

Source: https://exaly.com/author-pdf/2371312/publications.pdf Version: 2024-02-01



#	Article	IF	CITATIONS
1	Gallium-Doped Li ₇ La ₃ Zr ₂ O ₁₂ Garnet-Type Electrolytes with High Lithium-Ion Conductivity. ACS Applied Materials & Interfaces, 2017, 9, 1542-1552.	8.0	266
2	Photonic Potentiation and Electric Habituation in Ultrathin Memristive Synapses Based on Monolayer MoS ₂ . Small, 2018, 14, e1800079.	10.0	224
3	Synaptic Metaplasticity Realized in Oxide Memristive Devices. Advanced Materials, 2016, 28, 377-384.	21.0	210
4	Synaptic Suppression Triplet‣TDP Learning Rule Realized in Secondâ€Order Memristors. Advanced Functional Materials, 2018, 28, 1704455.	14.9	183
5	Garnet-Type Fast Li-Ion Conductors with High Ionic Conductivities for All-Solid-State Batteries. ACS Applied Materials & Interfaces, 2017, 9, 12461-12468.	8.0	179
6	MOF-derived nanoporous multifunctional fillers enhancing the performances of polymer electrolytes for solid-state lithium batteries. Journal of Materials Chemistry A, 2019, 7, 2653-2659.	10.3	160
7	In Situ Formed Shields Enabling Li ₂ CO ₃ -Free Solid Electrolytes: A New Route to Uncover the Intrinsic Lithiophilicity of Garnet Electrolytes for Dendrite-Free Li-Metal Batteries. ACS Applied Materials & Interfaces, 2019, 11, 898-905.	8.0	147
8	Ultraviolet photocatalytic degradation of methyl orange by nanostructured TiO ₂ /ZnO heterojunctions. Journal of Materials Chemistry A, 2015, 3, 6565-6574.	10.3	141
9	Memristive Synapses with Photoelectric Plasticity Realized in ZnO _{1–<i>x</i>} /AlO _{<i>y</i>} Heterojunction. ACS Applied Materials & Interfaces, 2018, 10, 6463-6470.	8.0	120
10	Hierarchical and Hollow Fe ₂ O ₃ Nanoboxes Derived from Metal–Organic Frameworks with Excellent Sensitivity to H ₂ S. ACS Applied Materials & Interfaces, 2017, 9, 29669-29676.	8.0	118
11	NO sensing by single crystalline WO3 nanowires. Sensors and Actuators B: Chemical, 2015, 219, 346-353.	7.8	110
12	Origin of the low grain boundary conductivity in lithium ion conducting perovskites: Li _{3x} La _{0.67â^x} TiO ₃ . Physical Chemistry Chemical Physics, 2017, 19, 5880-5887.	2.8	100
13	Nanostructured Metal–Organic Framework (MOF)â€Derived Solid Electrolytes Realizing Fast Lithium Ion Transportation Kinetics in Solidâ€State Batteries. Small, 2019, 15, e1804413.	10.0	93
14	Three-Dimensional Garnet Framework-Reinforced Solid Composite Electrolytes with High Lithium-Ion Conductivity and Excellent Stability. ACS Applied Materials & Interfaces, 2019, 11, 26920-26927.	8.0	87
15	Quasiâ€Hodgkin–Huxley Neurons with Leaky Integrateâ€andâ€Fire Functions Physically Realized with Memristive Devices. Advanced Materials, 2019, 31, e1803849.	21.0	87
16	Bio-inspired high-performance solid-state supercapacitors with the electrolyte, separator, binder and electrodes entirely from <i>kelp</i> . Journal of Materials Chemistry A, 2017, 5, 25282-25292.	10.3	85
17	Printable Zinc-Ion Hybrid Micro-Capacitors for Flexible Self-Powered Integrated Units. Nano-Micro Letters, 2021, 13, 19.	27.0	81
18	Hierarchical porous microspheres of activated carbon with a high surface area from spores for electrochemical double-layer capacitors. Journal of Materials Chemistry A, 2016, 4, 15968-15979.	10.3	80

#	Article	IF	CITATIONS
19	Silverâ€Quantumâ€Dotâ€Modified MoO ₃ and MnO ₂ Paperâ€Like Freestanding Films Flexible Solidâ€&tate Asymmetric Supercapacitors. Small, 2019, 15, e1805235.	for _{10.0}	79
20	Lotus pollen derived 3-dimensional hierarchically porous NiO microspheres for NO2 gas sensing. Sensors and Actuators B: Chemical, 2016, 227, 554-560.	7.8	77
21	Artificial Intelligence to Power the Future of Materials Science and Engineering. Advanced Intelligent Systems, 2020, 2, 1900143.	6.1	75
22	Electrospun Ni-doped SnO2 nanofiber array for selective sensing of NO2. Sensors and Actuators B: Chemical, 2017, 244, 509-521.	7.8	72
23	Bienenstock, Cooper, and Munro Learning Rules Realized in Secondâ€Order Memristors with Tunable Forgetting Rate. Advanced Functional Materials, 2019, 29, 1807316.	14.9	60
24	Hydrothermal degradation mechanism of tetragonal Zirconia. Journal of Materials Science, 2001, 36, 3737-3744.	3.7	59
25	<i>In situ</i> thermally polymerized solid composite electrolytes with a broad electrochemical window for all-solid-state lithium metal batteries. Journal of Materials Chemistry A, 2020, 8, 3892-3900.	10.3	59
26	Effects of potassium iodide (KI) on crystallinity, thermal stability, and electrical properties of polymer blend electrolytes (PVC/PEO:KI). Solid State Ionics, 2015, 278, 260-267.	2.7	57
27	Hierarchical flowerlike WO3 nanostructures assembled by porous nanoflakes for enhanced NO gas sensing. Sensors and Actuators B: Chemical, 2017, 246, 225-234.	7.8	57
28	Inorganic Solid Electrolytes for Allâ€Solidâ€State Sodium Batteries: Fundamentals and Strategies for Battery Optimization. Advanced Functional Materials, 2021, 31, 2008165.	14.9	55
29	Molybdenum trioxide nanopaper as a dual gas sensor for detecting trimethylamine and hydrogen sulfide. RSC Advances, 2017, 7, 3680-3685.	3.6	52
30	3D Porous Hierarchical Microspheres of Activated Carbon from Nature through Nanotechnology for Electrochemical Double-Layer Capacitors. ACS Sustainable Chemistry and Engineering, 2016, 4, 6463-6472.	6.7	51
31	An artificial olfactory inference system based on memristive devices. InformaÄnÃ-Materiály, 2021, 3, 804-813.	17.3	50
32	Pavlovian conditioning demonstrated with neuromorphic memristive devices. Scientific Reports, 2017, 7, 713.	3.3	49
33	Detecting low concentration of H2S gas by BaTiO3 nanoparticle-based sensors. Sensors and Actuators B: Chemical, 2017, 238, 16-23.	7.8	48
34	Multi-gate memristive synapses realized with the lateral heterostructure of 2D WSe ₂ and WO ₃ . Nanoscale, 2020, 12, 380-387.	5.6	47
35	Single crystalline flowerlike α-MoO3 nanorods and their application as anode material for lithium-ion batteries. Journal of Alloys and Compounds, 2016, 687, 79-86.	5.5	44
36	Near room temperature CO sensing by mesoporous LaCoO3 nanowires functionalized with Pd nanodots. Sensors and Actuators B: Chemical, 2016, 222, 517-524.	7.8	44

#	Article	IF	CITATIONS
37	NO2 sensing properties of SmFeO3 porous hollow microspheres. Sensors and Actuators B: Chemical, 2018, 265, 443-451.	7.8	41
38	Gigantically enhanced NO sensing properties of WO3/SnO2 double layer sensors with Pd decoration. Sensors and Actuators B: Chemical, 2015, 220, 398-405.	7.8	40
39	Flexible and transparent sensors for ultra-low NO ₂ detection at room temperature under visible light illumination. Journal of Materials Chemistry A, 2020, 8, 14482-14490.	10.3	39
40	Artificial Neural Networks Based on Memristive Devices: From Device to System. Advanced Intelligent Systems, 2020, 2, 2000149.	6.1	39
41	Cadmium removal in waste water by nanostructured TiO ₂ particles. Journal of Materials Chemistry A, 2014, 2, 13932-13941.	10.3	37
42	Mimicking the brain functions of learning, forgetting and explicit/implicit memories with SrTiO ₃ -based memristive devices. Physical Chemistry Chemical Physics, 2016, 18, 31796-31802.	2.8	36
43	Bio-templated fabrication of hierarchically porous WO ₃ microspheres from lotus pollens for NO gas sensing at low temperatures. RSC Advances, 2015, 5, 29428-29432.	3.6	31
44	LaCoO ₃ -based sensors with high sensitivity to carbon monoxide. RSC Advances, 2015, 5, 65668-65673.	3.6	31
45	Determination of electronic and ionic partial conductivities of a grain boundary: method and application to acceptor-doped SrTiO3. Solid State Ionics, 2002, 154-155, 563-569.	2.7	27
46	LaFeO3 porous hollow micro-spindles for NO2 sensing. Ceramics International, 2019, 45, 5240-5248.	4.8	25
47	Hybrid electrolytes with an ultrahigh Li-ion transference number for lithium-metal batteries with fast and stable charge/discharge capability. Journal of Materials Chemistry A, 2021, 9, 18239-18246.	10.3	25
48	Selfâ€Healing Polymer Electrolyte for Dendriteâ€Free Li Metal Batteries with Ultraâ€Highâ€Voltage Niâ€Rich Layered Cathodes. Small, 2022, 18, e2200891.	10.0	23
49	Defect Structure Modification in Zirconia by Alumina. Physica Status Solidi A, 2001, 183, 261-271.	1.7	22
50	Oxygen sensors based on SrTi0.65Fe0.35O3â^'δ thick film with MgO diffusion barrier for automotive emission control. Sensors and Actuators B: Chemical, 2015, 213, 102-110.	7.8	19
51	Characteristics and sensing properties of CO gas sensors based on LaCo 1â^'x Fe x O 3 nanoparticles. Solid State Ionics, 2017, 303, 97-102.	2.7	19
52	Behavioral Plasticity Emulated with Lithium Lanthanum Titanateâ€Based Memristive Devices: Habituation. Advanced Electronic Materials, 2017, 3, 1700046.	5.1	19
53	A Bioâ€Inspired Neuromorphic Sensory System. Advanced Intelligent Systems, 2022, 4, .	6.1	18
54	CO sensing mechanism of LaCoO3. Solid State Ionics, 2015, 272, 155-159.	2.7	17

#	Article	IF	CITATIONS
55	Integrated interface between composite electrolyte and cathode with low resistance enables ultra-long cycle-lifetime in solid-state lithium-metal batteries. Science China Chemistry, 2021, 64, 673-680.	8.2	16
56	A New Lithiumâ€lon Conductor LiTaSiO ₅ : Theoretical Prediction, Materials Synthesis, and Ionic Conductivity. Advanced Functional Materials, 2019, 29, 1904232.	14.9	15
57	Single crystalline SrTiO3 as memristive model system: From materials science to neurological and psychological functions. Journal of Electroceramics, 2017, 39, 210-222.	2.0	14
58	Electroformingâ€Free Artificial Synapses Based on Proton Conduction in αâ€MoO 3 Films. Advanced Electronic Materials, 2020, 6, 1901290.	5.1	14
59	Synthesis and characterization of one-dimensional metal oxides: TiO2, CeO2, Y2O3-stabilized ZrO2 and SrTiO3. Ceramics International, 2015, 41, 533-545.	4.8	13
60	SrTi0.65Fe0.35O3 nanofibers for oxygen sensing. Solid State Ionics, 2015, 278, 26-31.	2.7	11
61	Hierarchically-structured MnFe2O4 nanospheres for highly sensitive detection of NO2. Solid State lonics, 2019, 336, 102-109.	2.7	11
62	Oxygen pump based on stabilized zirconia. Review of Scientific Instruments, 2015, 86, 115103.	1.3	9
63	Ultravioletâ€Cured Semiâ€Interpenetrating Network Polymer Electrolytes for Highâ€Performance Quasiâ€Solidâ€State Lithium Metal Batteries. Chemistry - A European Journal, 2021, 27, 7773-7780.	3.3	8
64	Light-excited chemiresistive sensors integrated on LED microchips. Journal of Materials Chemistry A, 2021, 9, 16545-16553.	10.3	7
65	Insulator-to-semiconductor transition of nanocrystalline BaTiO ₃ at temperatures â‰200 °C. Physical Chemistry Chemical Physics, 2014, 16, 20420-20423.	2.8	6
66	Morphology engineering of nanostructured TiO ₂ particles. RSC Advances, 2015, 5, 6481-6488.	3.6	5
67	Memristive Devices with Multiple Resistance States Based on the Migration of Protons in αâ€MoO ₃ /SrCoO _{2.5} Stacks. Advanced Electronic Materials, 2021, 7, 2001243.	5.1	5
68	Solid Electrolytes: A New Lithiumâ€lon Conductor LiTaSiO ₅ : Theoretical Prediction, Materials Synthesis, and Ionic Conductivity (Adv. Funct. Mater. 37/2019). Advanced Functional Materials, 2019, 29, 1970253.	14.9	4
69	Artificial Intelligence to Power the Future of Materials Science and Engineering. Advanced Intelligent Systems, 2020, 2, 2070042.	6.1	3
70	A Pressure Responsive Artificial Interphase Layer of BaTiO ₃ against Dendrite Growth for Stable Lithium Metal Anodes. Batteries and Supercaps, 2022, 5, .	4.7	3
71	Proof of Concept for Operando Infrared Spectroscopy Investigation of Light-Excited Metal Oxide-Based Gas Sensors. Journal of Physical Chemistry Letters, 2022, 13, 3631-3635.	4.6	2
72	Structure and magnetic properties of highly oriented LaBaCo2O5+δfilms deposited on Si wafers with Pt/Ti buffer layer. Physical Chemistry Chemical Physics, 2019, 21, 22390-22395.	2.8	1

#	Article	IF	CITATIONS
73	Artificial Neurons: Quasiâ€Hodgkin–Huxley Neurons with Leaky Integrateâ€andâ€Fire Functions Physically Realized with Memristive Devices (Adv. Mater. 3/2019). Advanced Materials, 2019, 31, 1970020.	21.0	0
74	Singleâ€Ion Magnetostriction in Gd 2 O 3 –CeO 2 Solid Solutions. Advanced Functional Materials, 0, , 2110509.	14.9	0